

The drying shrinkage of cellulosic fibres and isotropic paper sheets

W. W. Sampson · J. Yamamoto

Received: 22 July 2010/Accepted: 12 October 2010/Published online: 27 October 2010
© Springer Science+Business Media, LLC 2010

Abstract We present theory for the shrinkage on drying of the cross-sectional area of cellulosic fibres and show that this depends on their initial moisture content only. For the linear shrinkage of cross-sectional dimensions, an additional parameter is required, which we estimate from comparison of the theory with experimental data from the literature. We proceed to combine our model of fibre shrinkage with probabilistic theory for fibre contacts in random fibrous networks to obtain a model for the unrestrained shrinkage of isotropic paper sheets. The expression obtained depends only on the moisture content of fibres and the extent of inter-fibre contact and exhibits good agreement with experimental data for laboratory-formed paper sheets. The results have relevance to the commercial manufacture of paper and potential for application to the study of cellulose nano-composites.

Introduction

The manufacture of paper involves the processing of aqueous suspensions of cellulosic fibres. In advance of the paper making process, fibres are typically subjected to mechanical action, in a process known as refining, to increase sheet density and hence strength via controlled damage of fibres. The major effects of refining, and its equivalent batchwise process, beating, are to induce

internal and external fibrillation, to generate fibre fragments, and to reduce the length of fibres. The fibre fragments generated during beating and refining are termed ‘fines’ and include micro-fibrillar cellulosics [1]. The process of forming paper is essentially one of water removal: after the sheet is formed in a continuous filtration process, water is removed and the sheet is consolidated in a pressing process before the remaining water is removed by drying. Recent reviews giving overviews of papermaking processes and discussing structure–property dependencies are provided by Alava and Niskanen [2] and Sampson [3].

In common with many materials, paper shrinks during drying. Given the directional nature of the sheet forming process, the sheet dries under tension in the direction of manufacture (MD) and thus is restrained from shrinkage in this direction. The direction perpendicular to the MD is called the cross-direction (CD); in this direction the sheet exhibits significant shrinkage with a profile. The profile arises because the web is unrestrained at the edges, so shrinks more there than at the centre, where it can be considered self-restrained [4].

The cross-direction shrinkage of paper is of significant interest to paper manufacturers since it affects paper properties [2, 4] and manufacturing efficiency [5]. As might be anticipated, the extent of shrinkage during manufacture influences the hygroexpansivity of the sheet [6, 7] and increases with the extent of inter-fibre contact [8]. We note also that when paper is exposed to cyclic moisture changes, hygroexpansion and shrinkage of fibres, coupled with the inherent structural heterogeneity of the sheet, result in a distribution of local stresses and hence stress gradients which accelerate mechano-sorptive creep phenomena [9].

Although commercially manufactured paper exhibits structural and mechanical anisotropy, the study of isotropic

W. W. Sampson (✉)
School of Materials, University of Manchester,
Manchester M13 9PL, UK
e-mail: w.sampson@manchester.ac.uk

J. Yamamoto
Nippon Paper Industries Co. Ltd, 5-21-1, Oji, Kita-ku,
Tokyo 114-0002, Japan

sheets formed in the laboratory is commonplace. Two recent results are of particular relevance in the context of this work:

- Regardless of fibre orientation distribution, the geometric mean shrinkage is constant and equal to the free shrinkage of an isotropic sheet [10].
- Although the shape of the CD shrinkage profile in paper is strongly influenced by the configuration of the press and dryer sections of the machine on which it is formed [11] the total amount of CD shrinkage depends also on the unrestrained shrinkage of the sheet in the machine and cross-machine directions [5].

Accordingly, better understanding of the factors affecting the unrestrained shrinkage of isotropic sheets will improve understanding of the shrinkage observed in commercial papermaking processes and should yield better estimates of the parameters used in models of CD shrinkage profiles.

Page and Tydeman [12] showed that when a single fibre dries without restraint, its length is almost unchanged, though it exhibits significant transverse shrinkage. They showed also that within sheets, longitudinal contraction of fibres is promoted at regions of fibre–fibre contact, and not in the free segments between contacts. Further, the longitudinal contraction of fibres was the same as the unrestrained shrinkage of the sheet. Thus, in unrestrained shrinkage, fibre shortening arises when the transverse shrinkage of one fibre causes longitudinal contraction of contacting fibres in bonded regions. Page and Tydeman suggested also that the free segments between contacts may shorten in response to the shrinkage forces acting at bond sites. Subsequently, Nanko et al. [13] observed no significant dimensional change in free segments of paper dried without restraint, and found that the observed shrinkage of the sheet was somewhat less than the longitudinal contraction of fibres.

Despite the importance of the shrinkage of fibres on that of the sheet, the literature contains limited data on the dimensional change of fibres when they are dried from a saturated state. Paulapuro and Weise [14] provide data giving the proportion of the swelling potential of pulps that is recoverable after repeated drying and rewetting, as experienced in repeated paper recycling processes, though do not provide fibre dimensions. Pulkkinen et al. [15] show a negative correlation between hygroexpansivity and fibre wall thickness, but do not provide data on shrinkage. Nanko and Wu [16] observed that the transverse shrinkage of thick-walled fibres was about double that of thin-walled fibres, but do not provide fibre dimensions.

Tydeman et al. [17] used calibrated radiography techniques to determine the width, ω (m), thickness, t (m) and moisture loss, M , of drying fibres in a sparse network, such

that their shrinkage in the width and thickness directions, S_ω and S_t , respectively, could be determined using

$$S_\omega = 1 - \frac{\omega_{\text{dry}}}{\omega_{\text{wet}}}; \quad S_t = 1 - \frac{t_{\text{dry}}}{t_{\text{wet}}}. \quad (1)$$

The data of Tydeman et al. for the shrinkages S_ω and S_t are plotted against the percentage moisture loss during drying in Fig. 1. The data include measurements made on unbeaten and heavily beaten chemically pulped softwood fibres. Note that Tydeman et al. reported data for some samples with free water such that the values of M were greater than 1; these data have been excluded from our analysis. We observe that typically $S_t > S_\omega$; linear regressions on the data, shown by the lines in Fig. 1, yield

$$S_\omega = 0.0091M \quad \text{with } r^2 = 0.596$$

$$S_t = 0.0043M \quad \text{with } r^2 = 0.385$$

such that $S_t \approx 2 S_\omega$. Tydeman et al. do not discuss these dependencies, though from their treatment of the data they observed that whereas there is no correlation between dry fibre thickness, t , and S_t , there is a negative correlation between dry fibre width, ω , and S_ω ; from consideration of the correlation coefficients, Tydeman et al. considered that about half the variability in shrinkage was attributable to variability in fibre width. We consider these data further in our subsequent analysis.

Given that longitudinal contraction of fibres occurs at regions of fibre contact, we expect the shrinkage of the network to be determined by the amount of contact between fibres and the extent to which the transverse shrinkage of one fibre results in axial compression of those fibres that it contacts. There is a considerable literature describing the fraction of fibre surface that is bonded to other fibres and much of this is reviewed by Batchelor and

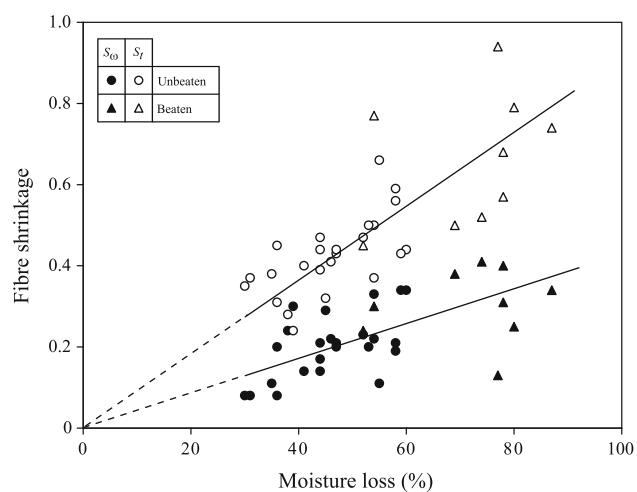


Fig. 1 Data of Tydeman et al. [17] showing width shrinkage, S_ω , and thickness shrinkage, S_t plotted against percentage moisture loss during drying under vacuum

co-workers [18–20]. When modelling fibre networks, the structural parameter of interest is the fraction of fibre surface that is in contact with other fibres. This ‘fractional contact area’, Φ , depends on the porosity of the network, ϵ and the fraction of fibres located in the surfaces of the network, and thus available for contact with other fibres on one side only [21]. The fraction of fibres in the surfaces of the network depends on the expected number of fibres covering points in the network, which we term the mean coverage, \bar{c} ; this parameter is given by

$$\bar{c} = \frac{\bar{\beta}}{\beta_f} = \frac{\bar{\beta}\omega}{\delta}, \quad (2)$$

where $\bar{\beta}$ is the mean mass per unit area, or areal density, of the sheet (kg m^{-2}), β_f is the areal density of fibres (kg m^{-2}) and δ is the linear density of the fibres (kg m^{-1}).

The fractional contact area of a random fibre network is given by [22, 23]

$$\Phi = \left(1 + \frac{\gamma - \text{Ei}(\bar{c}) + \log(\bar{c})}{e^{\bar{c}} - 1}\right) \left(1 - \frac{\epsilon(1 - \epsilon)(2 - \epsilon)}{\log(1/\epsilon)}\right) \quad (3)$$

where γ is Euler’s constant and $\text{Ei}(\bar{c})$ is the exponential integral function. Note that the derivation of Eq. 3 given in [22, 23] addresses an approximation in the original presentation of the theory given in [21].

The first term in parentheses on the right-hand side of Eq. 3 is the fraction of fibres in the surfaces of the network; the second term in parentheses is the probability that a pair of vertically adjacent fibres make contact [23, 22]. We have previously shown that this influences the mechanical properties of paper such that the specific tensile strength and specific elastic modulus increase with areal density, though for mechanical properties, scale effects must be considered also [24, 25].

Here we present a simple model for the shrinkage of fibres during drying and compare this with the results of Tydeman et al. [12]. Guided by this treatment, we propose a model for shrinkage of isotropic networks that takes account of fractional contact area. The results are compared with experimental data.

Fibre shrinkage

Consider a sample of saturated cellulose with moisture ratio, m , such that each gram of dry cellulose is associated with m grams of water. Denoting the density of cellulose, ρ_c and that of water, ρ_w , the saturated volume of a unit mass of dry cellulose is

$$V_{\text{wet}} = \frac{1}{\rho_c} + \frac{m}{\rho_w}. \quad (4)$$

After drying, the volume of the cellulose is, $V_{\text{dry}} = 1/\rho_c$, such that the volumetric shrinkage is

$$\begin{aligned} S_v &= 1 - \frac{V_{\text{dry}}}{V_{\text{wet}}} \\ &= \frac{m\rho_c}{m\rho_c + \rho_w} \end{aligned} \quad (5)$$

The specific gravity of cellulose is approximately 1.5, so $\rho_c \approx 3\rho_w/2$ and

$$S_v = \frac{3m}{2 + 3m}. \quad (6)$$

For an isotropic material, the linear shrinkage in any direction is given by

$$S_{\text{iso}} = 1 - (1 - S_v)^{\frac{1}{3}}. \quad (7)$$

We noted earlier that fibres exhibit minimal shrinkage along their length. Accordingly, if we assume this axial shrinkage to be zero, then Eq. 6 describes the shrinkage of the cross sectional area of fibres, S_a . This area shrinkage is related to the linear shrinkages in the width and thickness direction by

$$\begin{aligned} S_a &= 1 - \frac{\omega_{\text{dry}} t_{\text{dry}}}{\omega_{\text{wet}} t_{\text{wet}}} \\ &= 1 - (1 - S_\omega)(1 - S_t). \end{aligned} \quad (8)$$

Further, we expect the linear shrinkages in the width and thickness direction to be given by

$$\begin{aligned} S_\omega &= 1 - (1 - S_v)^n \\ &= 1 - \left(\frac{2}{2 + 3m}\right)^n, \end{aligned} \quad (9)$$

and

$$\begin{aligned} S_t &= 1 - (1 - S_v)^{1-n} \\ &= 1 - \left(\frac{2}{2 + 3m}\right)^{1-n}, \end{aligned} \quad (10)$$

respectively, where $0 < n \leq 1$ and substitution of Eqs. 9 and 10 in Eq. 8 yields $S_a = S_v$. Note that if shrinkage in the cross-sectional dimensions is isotropic, then $S_\omega = S_t$ and $n = 1/2$. The data presented in Fig. 1 show anisotropic shrinkage of the cross-sectional dimensions with S_t typically greater than S_ω ; to satisfy this criterion we require $0 < n < 1/2$.

To estimate the value of parameter n , we turn to the data of Tydeman et al. [17] and use empirical methods. Although Tydeman et al. did not report values of S_a , these can be calculated from their data for S_ω and S_t using Eq. 8.

Comparison with experimental data

Figure 2 shows the shrinkage data of Tydeman et al. [17] for S_ω and S_t and S_a calculated from these using Eq. 8,

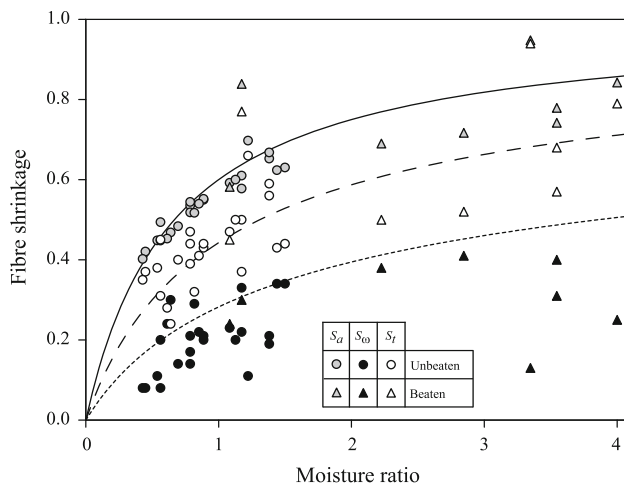


Fig. 2 Data of Tydeman et al. [17] showing width shrinkage, S_ω , and thickness shrinkage, S_t and shrinkage of cross-sectional area, S_a , calculated using Eq. 8 plotted against moisture ratio. The lines represent Eq. 6 and Eqs. 9 and 10 with $n = 1/3$, as discussed in the text

plotted against the moisture ratio, $m = M/(1 - M)$. The solid line represents $S_a = S_v$ as given by Eq. 6. For the unbeaten fibres, Fig. 2 shows excellent agreement between Eq. 6 and the data for the shrinkage of the cross-sectional area of fibres, S_a ; for the beaten fibres there is some difference between the data and the curve, though we note that the general trend of the data is consistent with the theory.

The agreement between the data for S_a and Eq. 6 shown in Fig. 2, is supportive of our assumption that axial shrinkage of fibres is negligible. A least-squares fit of Eq. 10 to the data for S_t plotted in Fig. 2 yields $n = 0.638$ with $r^2 = 0.974$; fitting to the data for the unbeaten fibres only yields $n = 0.670$ with $r^2 = 0.973$. For simplicity in our subsequent application of Eq. 9, we assume that $n = 1/3$. Curves for Eqs. 9 and 10 with $n = 1/3$ are represented by the dotted and dashed lines in Fig. 2, respectively.

Substituting the values of m calculated from the data of Tydeman et al. [17] into Eq. 6 and Eqs. 9 and 10 with $n = 1/3$, allows prediction of the shrinkages S_a , S_ω and S_t , respectively. These values are plotted against the shrinkage data of Tydeman et al. [17] in Fig. 3 where the broken line has unit gradient. A linear regression with intercept at the origin has gradient 1.04 with $r^2 = 0.847$.

As was clear from Fig. 2, the agreement between theory and experiment shown in Fig. 3 is closest for the area shrinkage of unbeaten pulps. We observe also that there is considerable scatter for the data for S_ω and for all the data associated with beaten fibres. We note that the beaten fibres had been subjected to a very heavy beating¹ such that the

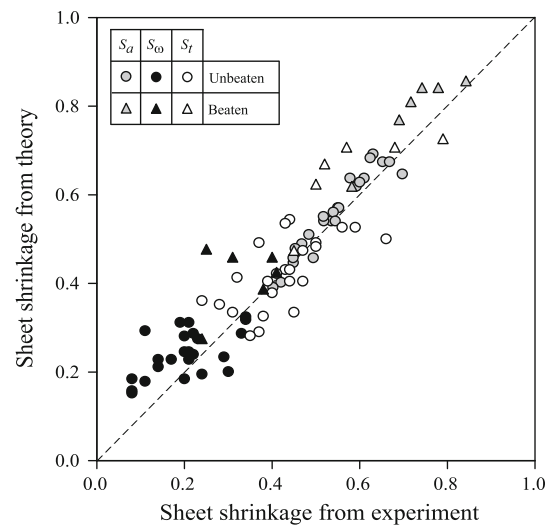


Fig. 3 Fibre shrinkages S_a , S_ω and S_t as predicted by Eqs. 6, 9 and 10 with $n = 1/3$ plotted against the shrinkage data of Tydeman et al. [17]. The *broken line* has unit gradient

fibres are not representative of those used to manufacture most paper grades. The scatter associated with the data for S_ω should be considered in association with that obtained for S_t . Scatter in these data is inevitable considering the inherent variability in natural fibres. Our treatment suggests that whereas the area shrinkage of fibres depends only on their moisture content, the change in cross-sectional dimensions of individual fibres in the two principal directions can vary considerably, presumably as a consequence of their differing morphology and anisotropy of elastic moduli. We note that there is no correlation between S_t and S_ω for the data of Tydeman et al. [17]. Since the number of fibres in the network is always sufficiently large that their average shrinkage behaviour will adequately characterise the contribution of fibre properties to those of the sheet, variability among fibres should not concern us when inferring sheet shrinkage from fibre properties. Accordingly, we consider Eqs. 6–9 with $n = 1/3$ to provide, at least to a first approximation, sensible predictions of the shrinkages in the cross-sectional dimensions of fibres during drying.

Network shrinkage

Given that shrinkage of the network arises from axial compression of fibres at regions of contact with other fibres [12, 13] we expect the shrinkage of the network, S_n , to be proportional to the fraction of fibre surface in contact with other fibres, Φ , and their width shrinkage, S_ω . When two fibres cross with angle θ , the component of the transverse shrinkage of one fibre that can induce axial compression of

¹ The Schopper–Riegler wetness, a widely used measure of the extent of beating, was 85°.

the other is $S_\omega \sin(\theta)$. For an isotropic network of fibres, the average value of $\sin(\theta)$ is $\pi/4$ [23], so we have

$$S_n = \frac{k\pi S_\omega \Phi}{4}, \quad (11)$$

where k is a constant. The network shrinkage, S_n , is effectively a negative strain, so we expect k to depend on the efficiency of stress-transfer in regions of inter-fibre contact and the axial moduli of fibres. Note that both these properties are expected to depend on the moisture content of fibres and hence that of the network, so they will vary during drying. Accordingly, $0 \leq k \leq 1$ quantifies the total axial compression of fibres as a fraction of the transverse shrinkage of fibres in regions of inter-fibre contact over the drying process.

Substitution of Eqs. 3 and 9 with $n = 1/3$ into Eq. 11 yields our final expression for the shrinkage of the network:

$$S_n = \frac{k\pi}{4} \left(1 + \frac{\gamma - Ei(c) + \log(c)}{e^c - 1} \right) \left(1 - \frac{\epsilon(1-\epsilon)(2-\epsilon)}{\log(1/\epsilon)} \right) \times \left(1 - \left(\frac{2}{2+3m} \right)^{\frac{1}{3}} \right). \quad (12)$$

Comparison with experimental data

Equation 12 gives the network shrinkage, S_n , as a function of the mean coverage of the network \bar{c} , its porosity, ϵ , and the moisture content of the fibres, m . To test Eq. 12, we formed isotropic paper sheets in the laboratory and measured their unrestrained shrinkage. The mean coverage of the sheets, \bar{c} , was altered by changing their areal density (cf. Eq. 2). Sheet porosity was altered by introducing a controlled fraction of fines to the network and thus increasing their density. The saturated moisture content of fines is known to be greater than that of fibres [26], so by varying fines content, we varied parameter m also. Full details of the experimental method have been published recently elsewhere [27], so here we provide a summary of the pertinent points only.

A once-dried bleached kraft pine pulp was soaked for 24 h and beaten for 20 min in the Valley beater. Fines were removed from the resulting pulp by screening with a Somerville fractionator fitted with an 80 mesh screen and collecting the retained fibre; we refer to this pulp as being ‘fines-free’. A second batch of pulp was beaten for 2 h in the Valley beater and from this the fines were isolated by screening with a Somerville fractionator and collecting the material that passed through a 200 mesh screen on a clean muslin cloth.

Some preliminary experiments were carried out to determine the retention of the fines-free pulp and that of fines by an evolving network of these fibres. From this initial characterisation, we were able to carefully control

the fractions of fibres and fines in the sheets. Sheets with grammage between 20 and 120 g m⁻² were formed from the fines-free pulp and from the fines-free pulp blended with 10% and 20% fines. Their unrestrained shrinkage was determined by measuring the distance after drying between two marks made on the wet sheet (TAPPI T-205 sp-05). Sheets containing between 5 and 30% fines were formed with areal density 60 g m⁻². In addition to making sheets for analysis of shrinkage, standard sets of sheets were made and dried under restraint. The values of areal density, thickness, and density reported here arise from measurements on these samples.

To determine the saturated moisture content, m , further sheets were made containing up to 70% fines and their water retention value was determined by centrifugation. The water retention value of the fines-free pulp was 2.26. A plot of water retention value against fines content was highly linear ($r^2 = 0.979$), indicating that the water retention value of a blend of fibres and fines obeys a simple rule of mixtures. Extrapolation from the linear regression indicated that the water retention value of the fines was 4.20, i.e. about double that of the fibres, in agreement with the observations of Laivins and Scallan [26].

Analysis of our fines-free pulp using a Metso Fiberlab analyser (Metso Automation, Kajaani, Finland) gave the linear density of fibres as 2.1×10^{-7} kg m⁻¹ and the mean fibre width, in the wet state, as 27 µm. The ratio of the width of a hollow cylindrical fibre to that of a ribbon-like fibre, assuming they both have the same fibre wall thickness and perimeter, is approximately $\pi/2$, so we estimate that after pressing and before drying, the fibre width was about 42 µm, such that the areal density of a fibre on a dry basis was, $\beta_f = \delta/\omega = 5$ g m⁻².

The areal density of the samples was determined gravimetrically and their thickness was measured using an electronic micrometer (ISO 5270:1999). Since paper is a compressible material with irregular surfaces, the ratio of areal density to thickness increases with areal density and is termed the ‘apparent density’. The true density, or ‘intrinsic density’, of our samples with different areal densities can be determined as the gradient of a plot of the areal density against the thickness, which typically has a non-zero intercept [28, 29].

For the sheets formed with 0, 10 and 20% fines, plots of areal density against thickness all exhibited $r^2 > 0.997$, indicating that the intrinsic density was independent of areal density for a given fines content. This is reassuring, since it validates the experimental procedures used to control the fines fraction retained in the sheets. For the sheets formed with 5, 15, 25 and 30% fines the areal density was fixed at 60 g m⁻², so the intrinsic density could not be determined by regression, though their apparent density was known. Accordingly, the intrinsic densities of these samples were

Table 1 Apparent densities (60 g m^{-2} sheets) and intrinsic densities for sheets with different fines contents

| Fines content (%) | Apparent density (kg m^{-3}) | Intrinsic density (kg m^{-3}) |
|-------------------|---|--|
| 0 | 587 | 574 |
| 5* | 632 | 650 |
| 10 | 715 | 792 |
| 15* | 726 | 804 |
| 20 | 791 | 907 |
| 25* | 792 | 912 |
| 30* | 826 | 968 |

Intrinsic densities for samples marked with an asterisk were determined from a linear regression on the data with no asterisk

calculated from a linear regression on the data for the apparent density and intrinsic density of the samples with 0, 10 and 20% fines ($r^2 = 0.999$). The densities of the samples are given in Table 1.

The unrestrained shrinkage of sheets containing 0, 10 and 20% is plotted against areal density in Fig. 4. The solid lines represent a least-squares fit of Eq. 12 to the data. For fitting purposes, the porosity, ϵ , was calculated from the intrinsic density, ρ :

$$\epsilon = 1 - \frac{\rho}{\rho_c}. \quad (13)$$

The coverage was calculated by modifying Eq. 2 to take account of the fraction of fines, f , such that

$$\bar{c} = \frac{(1-f)\bar{\beta}}{\beta_f}. \quad (14)$$

The value of $\beta_f = 5 \text{ g m}^{-2}$ was used, as discussed previously. The moisture ratio, m , was determined by applying a simple rule of mixtures to the experimentally determined

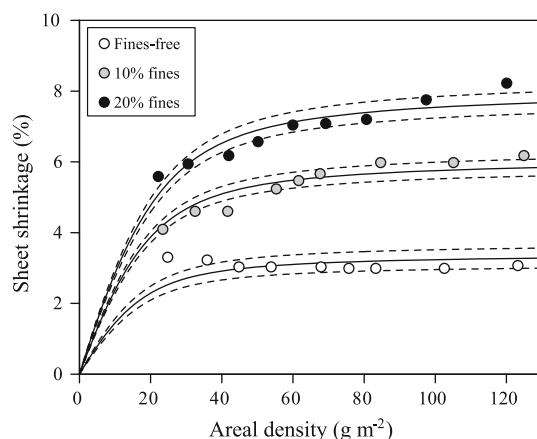


Fig. 4 Network shrinkage plotted against areal density. Solid lines represent a least-squares fit of Eq. 12 to the data; broken lines represent 95% confidence intervals on the fitted curves

Table 2 Curve-fitting parameters arising from least-squares fits of Eq. 12 to the data shown in Fig. 4

| Fines content (%) | Parameter k | r^2 |
|-------------------|-------------------|-------|
| 0 | 0.346 ± 0.030 | 0.989 |
| 10 | 0.392 ± 0.016 | 0.997 |
| 20 | 0.423 ± 0.017 | 0.998 |

water retention values of the fines-free pulp and fines. Accordingly, the only free parameter for fitting was the constant, k . Values of parameter k , including 95% confidence limits and the coefficient of determination, r^2 , arising from the least-squares fits, are given in Table 2; the broken lines in Fig. 4 represent 95% confidence limits on the fitted curve.

In the case of the sheets formed from the fines-free pulp, the data exhibited a weak initial decrease with areal density, so the fitted curve inevitably does not pass through the data for low areal densities. For the sheets containing 10% fines agreement between theory and data is good. Arguably, a straight line would give a good approximation of the data for the sheets containing 20% fines, though this would give a positive intercept on the ordinate, which is not justifiable in a physical context. Instead, as the areal density of the sheet tends towards zero, then so should the free shrinkage, since the number of contacts for transverse shrinkage of fibres to induce axial contraction of fibres diminishes. Accordingly, although the shape of the theoretical curve does not precisely match that of the data for the sheets containing 20% fines, the agreement is generally good.

Statistical analysis of the values of k given in Table 2 shows that there is no significant difference at the 0.05 level between the values of k for the sheets containing 10% and 20% fines, though these are significantly different at the same level from the value obtained for the fines-free sheets. The values of k given in Table 2 suggest that for our pulps, the axial compression of fibres in regions of inter-fibre contact is about 40% of the transverse shrinkage of fibres when fines are present, and about 35% when they are not.

On this basis, we applied Eq. 12 to predict the unrestrained shrinkage of sheets with differing fines contents and mean areal density 60 g m^{-2} . Again, we used Eq. 14 to determine the mean coverage of the sheets and applied a simple mixing rule to determine the value of m ; porosity was calculated from the intrinsic densities given in Table 1. For the fines-free sample, we used the value of k from Table 2; for the samples containing fines, we assumed k to be constant and equal to the mean of the values for samples containing 10% and 20% fines, as given in Table 2. Comparison between experimental data and the values obtained using Eq. 12 is given in Fig. 5 where the broken line has unit gradient. The data for fines contents up

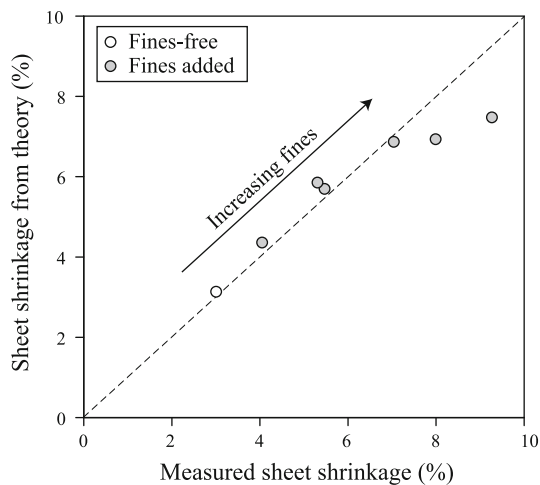


Fig. 5 Sheet shrinkage calculated from Eq. 12 plotted against that measured for sheets with fines contents between 5 and 30%. The broken line has unit gradient

to 20% are close to this line, though the model slightly underestimates the shrinkage observed for the samples containing 25 and 30% fines; this underestimate could be due to the use of a single value of k for all the sheets containing fines. Further experimental work would be required to determine if k increases with fines content over the full range considered here. Overall however, the model can be considered to be giving good prediction of unrestrained shrinkage for the range of fines contents observed in typical papermaking processes.

Conclusions

We have presented theory that relates the shrinkage of the cross-sectional dimensions of cellulosic fibres during drying to their initial moisture content. Comparison of the model with data from the literature shows excellent agreement for the shrinkage of the cross-sectional area of fibres. Although there is more scatter when experimental data for the shrinkage of fibre width and thickness are compared with the model, we attribute this to the inherent variability of natural fibres and consider the model to give a good prediction of the average shrinkage of these dimensions.

On this basis, and using an empirically determined exponent in our model of fibre shrinkage we have proposed that the shrinkage of isotropic networks is proportional to the width shrinkage of fibres and the fraction of fibre surface in the network that is in contact with other fibres. This treatment shows good agreement with experimental data for laboratory-formed paper sheets and suggests that for our samples the axial compression in regions of inter-fibre contact is about 40% of the transverse shrinkage of fibres when fines are present and about 35% when they are not.

The results have relevance to the commercial manufacture of paper, where network shrinkage perpendicular to the direction of manufacture is known to depend on the potential shrinkage of an isotropic sheet. We note also that shrinkage has been identified in cellulosic nano-composites [30], and that our treatment may have relevance to such materials.

References

- Subramanian R, Kononov A, Kang T, Paltakari J, Paulapuro H (2008) Bioresources 3(1):192
- Alava M, Niskanen K (2006) The physics of paper. Rep Prog Phys 69(3):669
- Sampson WW (2009) Int Mater Rev 54(3):134
- Phillips BR, I'Anson SJ, Hoole SM (2002) Appita J 55(3):235
- Constantino RPA, I'Anson SJ, Sampson WW (2005) In: I'Anson SJ (ed) Advances in paper science and technology. Trans. XIIIth Fund. Res. Symp, FRC, Manchester, p 283
- Uesaka T, Moss C, Nanri Y (1992) J Pulp Paper Sci 18(1):11
- Salmén L, Boman R, Fellers C, Htun M (1987) Nord Pulp Paper Res J 2(4):127
- Uesaka T (1994) J Mater Sci 29(9):2372. doi:[10.1007/BF00363429](https://doi.org/10.1007/BF00363429)
- Habeger CC, Coffin DW (2000) J Pulp Paper Sci 26(4):145
- Wahlström T (2009) In: I'Anson SJ (ed) Advances in pulp and paper research, Oxford 2009. Trans. XIVth Fund. Res. Symp, FRC, Manchester, p 1039
- Wahlström T, Lif JO (2003) In: Tappi international paper physics conference, Victoria. Tappi Press, Atlanta, p 169
- Page DH, Tydeman PA (2003) In: Bolam F (ed) Formation and structure of paper, Trans. IIInd Fund. Res. Symp. Oxford, 1961. FRC, Manchester, p 397
- Nanko H, Asano S, Oshawa J (1991) In: Proceedings of Tappi international paper physics conference. Kona, Hawaii, p 103
- Paulapuro H, Weise U (1999) J Pulp Paper Sci 25(5):163
- Pulkkinen I, Fiskari J, Alopaeus V (2009) Bioresources 4(1):126
- Nanko H, Wu J (1995) In: Proceedings of Tappi paper physics conference. Niagara-on-the-Lake, Canada, p 103
- Tydeman PA, Wembridge DR, Page DH (2003) In: Bolam F (ed) Consolidation of the paper web, Trans. IIIrd Fund. Res. Symp, Cambridge, 1965. FRC, Manchester, p 119
- Batchelor W, He J (2005) Tappi J 4(6):23
- Batchelor WJ, Kibblewhite RP (2006) Holzforschung 60(3):253
- He J, Batchelor WJ, Johnston RE (2007) J Mater Sci 42(2):522. doi:[10.1007/s10853-006-1146-9](https://doi.org/10.1007/s10853-006-1146-9)
- Sampson WW (2004) J Mater Sci 39(8):2775. doi:[10.1023/B:JMSC.0000021453.00080.5a](https://doi.org/10.1023/B:JMSC.0000021453.00080.5a)
- Sampson WW (2008) J Pulp Paper Sci 34(2):91
- Sampson WW (2009) Modelling stochastic fibrous materials with *Mathematica*. Springer-Verlag, London
- I'Anson SJ, Sampson WW (2007) Compos Sci Technol 67(7): 1650
- I'Anson SJ, Sampson WW, Savani S (2008) J Pulp Paper Sci 34(3):182
- Laijins GV, Scallan AM (1996) J Pulp Paper Sci 22(5):178
- Sampson WW, Yamamoto J (2010) Appita J (in press)
- Fellers C, Andersson H, Hollmark H (1986) In: Bristow JA, Kolseth P (eds) Paper structure and properties. Marcel Dekker, New York
- Sung YJ, Ham CH, Kwon O, Lee HL, Keller DS (2005) In: I'Anson SJ (ed) Advances in paper science and technology. Trans. XIth Fund. Res. Symp. FRC, Manchester, p 961
- Duchemin BJC, Newman RH, Staiger MP (2009) Compos Sci Technol 69(7–8):1225